Crustal Softening at Propagating Rift Tips, East Africa

F. Kolawole, R. Ajala

Lamont-Doherty Earth Observatory of Columbia University, 61 Rte 9W, Palisades, NY 10964

Corresponding author: Folarin Kolawole (fola@ldeo.columbia.edu)

Key Points:

- Earthquakes cluster at the rift tips within a zone of distributed faulting in exposed crystalline basement
- Highest Vp/Vs ratio anomalies occur at the modern and paleo- rift tips, collocated with thermal anomalies
- Localization of upper crustal brittle damage and thermal-weakening on a rift tip likely indicate initiation of lateral rift propagation

Abstract

We investigate the upper-crustal structure of the Rukwa-Tanganyika Rift Zone, East Africa, where earthquakes anomalously cluster at the northwestern tip of the Rukwa Rift, the eastern tip of the Mweru-Wantipa Rift, and along the Tanganyika Rift axis. The current rift tips host distributed faulting in exposed basement with little sedimentation. Here, we invert earthquake P and S travel times for three-dimensional upper-crustal velocity models for the region. The highest Vp/Vs ratios occur at the Rukwa and Mweru-Wantipa rift tips, and near a paleo-rift tip along an exhumed intra-basement shear zone beneath the Rukwa Rift. Colocated distributed faulting, upper-crustal seismicity, and thermal anomalies with high Vp/Vs ratios suggest a weakened crust at the rift tips. We propose an ongoing strain localization and crustal softening at the rift tips, accommodated by brittle damage and hydrothermal weakening of the crust, potentially representing a precursory phase that may initiate unilateral rift tip propagation.

Plain Language Summary

Continental rift systems evolve by the lateral propagation, interaction, linkage, and coalescence of isolated rift segments. Before linkage, interacting rift segments are separated by an elevated region of exposed crystalline basement with little to no sediment cover. This exposed basement area is progressively dismembered and down-thrown by the lateral propagation of faulting at the rift tips and subsidence of rift hanging walls. However, a long-standing question remains on how strain is localized onto rift tips to facilitate the basement deformation ahead of the rift basin. Here, we generate 3-D velocity models of the Rukwa-Tanganyika Rift Zone, a region where earthquakes anomalously cluster at rift tips. Our results reveal that most upper-crustal areas with low shear wave velocity (Vs) and anomalously high compressional-to-shear wave velocity ratio (Vp/Vs) occur at rift tips and are collocated with distributed faulting and geothermal anomalies. These anomalies indicate localized zones of fluid-saturated fractured crystalline basement. Thus, we suggest that at the rift tips, the upper crust is undergoing mechanical weakening by seismogenic brittle damage and hydrothermal processes. We argue that focused tectonic strain at the rift tip potentially represents a deformation phase that will facilitate the unilateral propagation of the rift into new areas.

Keywords:

Continental rift, rift propagation, earthquake tomography, normal fault, brittle deformation

1 Introduction

Inelastic deformation in regions of active tectonic extension manifests by tectonic and magmatic deformation of the crystalline crust and its overlying sedimentary sequences in the rift basins (e.g., Brune et al., 2023; Pérez-Gussinyé et al., 2023). Active tectonic deformation in continental rifts is commonly accommodated by widespread brittle deformation of the crust through faulting and fracturing and accompanied by earthquakes (e.g., Muirhead et al., 2019; Kolawole et al., 2017, 2018; Gaherty et al., 2019; Zheng et al., 2020; Stevens et al., 2021). The rift-bounding and intra-rift fault zones localize multi-scale fragmentation and communition of the rocks, allowing for progressive crustal stretching along weak deep-reaching faults (e.g., Brune et al., 2023 and references therein). The temporal, lateral propagation of the rift deformation into the intervening unrifted regions separating the rift basins progressively evolves the rift system towards break-up (e.g., Brune et al., 2023; Nelson et al., 1992; Zwaan et al., 2016; Zwaan & Schreurs, 2020; Kolawole et al., 2021a).

Fault-related damage and distributed brittle deformation in the crystalline crust often create regions of decreased bulk crustal density, manifested as anomalously low seismic shear wave velocity and high compressional-to-shear wave velocity ratio (Vp/Vs) zones (Allam et al., 2014; Fang et al., 2019). Also, regions where brittle damage allows the upwelling of hydrothermal fluids in the upper crust are associated with relatively higher Vp/Vs values (Hua et al., 2019). In active rift settings where surface volcanism is lacking, understanding the spatial distribution of upper-crustal seismic velocities permits identifying mechanically-weakened zones where tectonic strain may be preferentially localizing. Delineating these near-surface seismic velocity structures will help better predict ground motion amplification during large earthquake (Ajala & Persaud, 2021; Cormier & Spudich, 1984).

This contribution investigates how the earth's crystalline crust accommodates and localizes tectonic strain during continental rift propagation. We utilize recently acquired seismic data to explore the upper crustal structure of the Rukwa-Tanganyika Rift Zone, an active magma-poor rift zone along the East African Rift System, where previous studies have suggested a thick, strong, cold lithosphere (Craig et al., 2011; Foster & Jackson, 1998; Yang & Chen, 2010; Hodgson et al., 2017; Lavayssière et al., 2019) and ongoing unilateral propagation of the rift tips (Kolawole et al., 2021). A previous study (Hodgson et al., 2017) utilized the receiver function technique to map the spatial distribution of crustal-averaged Vp/Vs ratios but lacked constraints on the shallowest structure. Our results provide insight into the fundamental mechanism of strain distribution and localization along actively propagating rift segments. Ultimately, the approach may advance our understanding of how incipient divergent plate boundaries mature within active continental environments.

1.1 The Rukwa-Tanganyika Rift Zone

1.1.1 Pre-Rift Crystalline Basement

The crystalline crust of the Rukwa-Tanganyika Rift Zone (Fig. 1a) is mainly composed of metamorphic and igneous rocks of the Paleoproterozoic (1.85–1.95 Ga) Ubendian mobile belt (Fig. 1b). In the southwest, the Archean crystalline rocks of the Bangweulu Craton and its overlying Neoproterozoic sedimentary sequences dominate the basement (Fig. 1b). The Ubendian Belt consists of several amalgamated NW-trending terranes defining the orogenic belt that accommodated the Paleoproterozoic collision events (2.025–2.1 Ga) between the Archean

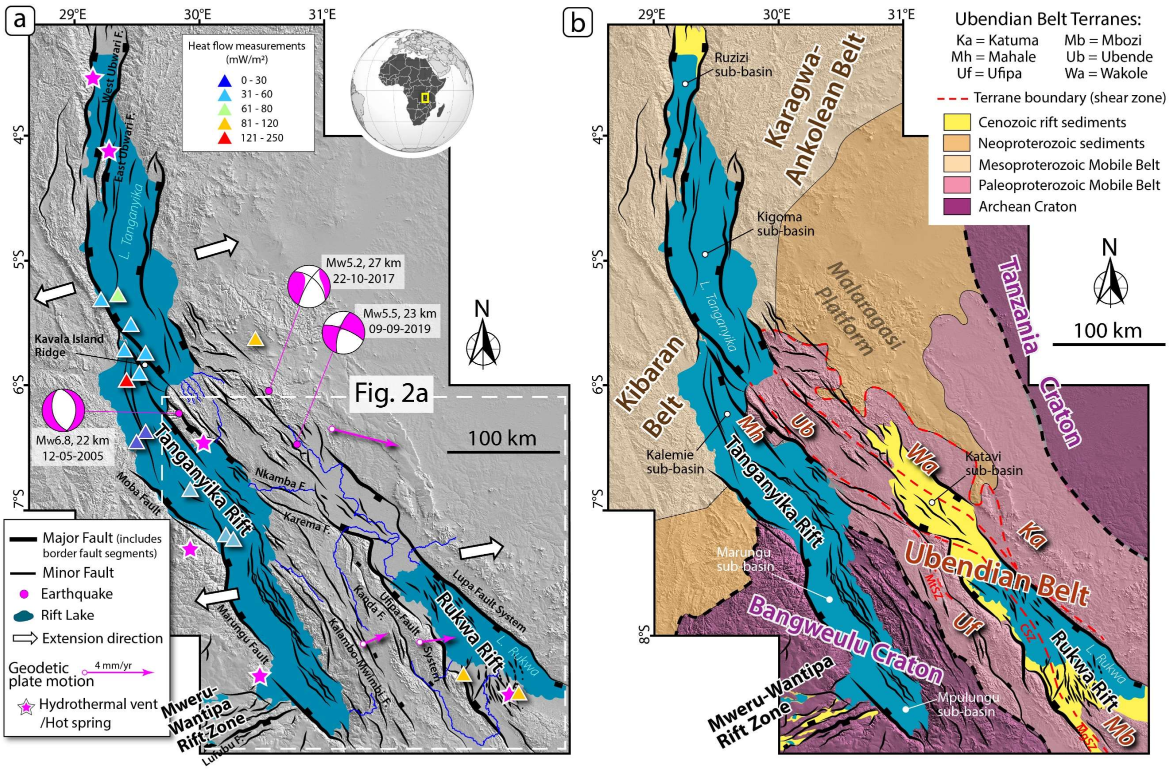

Figure 1. (**a**) Tectonic map of the Rukwa-Tanganyika Rift Zone showing the rift faults (Morley et al., 1999; Muirhead et al., 2019; Kolawole et al., 2021a). Mw >5 earthquake epicenters are from the USGS, and the focal mechanisms are from the Global CMT catalog (Ekstrom et al., 2012). Geodetic plate velocity data are from Stamps et al. (2008). Regional extension directions are from Delvaux and Barth (2010) for the northern Tanganyika Rift and Lavayssière et al. (2019) for the southern Tanganyika and Rukwa rift basins. Heat flow measurements and their locations are from Jones (2020). Sites of hot springs/hydrothermal vents are from Tiercelin et al. (1993), Lavayssière et al. (2019), Jones (2020), and Mulaya et al. (2022). (**b**) Geological map of the region, showing the cratons, mobile belts, terranes of the Ubendian Belt and shear zones, and Cenozoic syn-rift sediments (modified after Hanson, 2003; Delvaux et al., 2012; Kolawole et al., 2021a,b; Ganbat et al., 2021). Exhumed Precambrian shear zones (Heilman et al., 2019): CSZ, Chisi Shear Zone; MgSZ, Mughese Shear Zone; MtSZ: Mtose Shear Zone.

Tanzania Craton and the Bangweulu Block. The terranes, comprising Ufipa, Katuma, Wakole, Lupa, Mbozi, Ubende, and Upangwa (Fig. 1b; Daly, 1988; Lenoir et al., 1994), are now exhumed due to long-term erosion and are bounded by steeply-dipping, ductile, amphibolite facies, strike-slip shear zones (Fig. 1b; Daly, 1988; Lenoir et al., 1994; Theunissen et al., 1996; Kolawole et al., 2018, 2021b; Lemna et al., 2019; Heilman et al., 2019; Ganbat et al., 2021). Their associated ductile fabrics and bounding shear zones, commonly observed in basement exposures and aeromagnetic data, are suggested to have influenced the development of Phaneoroic rift basins in the region (Wheeler and Karson, 1994; Theunissen et al., 1996; Klerkx et al., 1998; Boven et al., 1999; Heilman et al., 2019; Lemna et al., 2019; Kolawole et al., 2018, 2021a,b).

1.1.2 Phanerozoic Rifting History

The Rukwa-Tanganyika Rift Zone is defined by a system of NNW-to-NW-trending overlapping rift segments, consisting of the Tanganyika Rift, the Rukwa Rift to its southeast, and the ENE-trending Mweru-Wantipa Rift located just southwest of its southernmost sub-basin (Fig. 1). The rift zone records multiple phases of Phanerozoic tectonic extension, with the first phase occurring in the Late Permian to Triassic, the second phase beginning in the Late Jurassic but peaking in the Cretaceous, and the third phase initiating in the Late Oligocene and presently persisting (e.g., Delvaux, 1989, Roberts et al., 2012). Although studies show that all the rift segments are currently active (e.g., Daly et al., 2020; Hodgson et al., Lavayssiere et al., 2019; Heilman et al., 2019; Kolawole et al., 2021a), available data indicate that they do not all record the three phases of Phanerozoic rifting (Delvaux, 1989).

Significant sedimentation and faulting in the Rukwa Rift (e.g., Morley et al., 1992, 1990) and colinear Luama Rift (Veatch, 1935; Delvaux, 1991; Kolawole et al., 2021b) characterize the Permo-Triassic (‘Karoo’) rift phase. The Cretaceous rifting event also included reactivated faulting, tectonic subsidence, and sedimentation in the Rukwa Rift and Luama Rift (e.g., Veatch, 1935; Delvaux, 1991; Roberts et al., 2012). Cenozoic rifting initiated the development of rift basins as segments of the ‘East African Rift System,’ featuring the reactivation of the Rukwa Rift and the development of the Tanganyika and the Mweru-Wantipa rift segments (e.g., Morley et al., 1999; Delvaux et al., 2001; Chorowicz, 2005; Daly et al., 2020). The current regional extension direction is N74°E in the northern Tanganyika Rift (Delvaux and Barth, 2010) and N80°E in the southern Tanganyika and Rukwa rifts (Lavayssière et al., 2019) (Fig. 1a).

1.1.3 Rift Faulting and Seismicity Patterns

The Tanganyika Rift basin is bounded by a system of large border faults that alternate polarity along-trend of the basin (Versfelt and Rosendahl, 1989) and include the Marungu Fault, the Kavala Island Ridge Faults, the West and East Ubwari Faults, and the Moba Fault (Fig. 1a). Whereas, the large graben of the Rukwa Rift basin is bounded by laterally continuous border fault systems of the Lupa Fault to the northeast and Ufipa Fault to the southwest (Heilman et al., 2019). The Ufipa Horst represents the intervening basement block between the southern Tanganyika Rift and the Rukwa Rift and is accommodating active deformation as evidenced by the ca. 100-km long scarps of the Kanda and Kalambo-Mwimbi Faults (Fig. 1a; Delvaux et al., 2012; Kolawole et al., 2021). Moreover, two prominent fault scarps extend westward from the Rukwa Rift tip across a basement region to the eastern margins of the central Tanganyika Rift (Nkamba and Karema Faults; Fig. 1a). The deformation zone of the Mweru-Wantipa Rift hosts a ca. 50-km-wide parallel fault cluster that defines its southeastern margin within which the Lufuba Fault appears to have the greatest escarpment height (Fig. 1a).

The entire Rukwa-Tanganyika Rift Zone records widespread seismicity (Figs. 2a, c–d) that extends beyond 42 km depth, indicating that the seismogenic layer of the rift includes the uppermost mantle (Fig. 2c–e; Lavayssière et al., 2019). The events define clusters with focal mechanism solutions that suggest steep, deep-rooting large normal faults (Lavayssière et al., 2019), and highlight localized active crustal deformation zones beneath Tanganyika Rift, Rukwa Rift, the Ufipa Horst, and the Mweru-Wantipa Rift (Fig. 1a). Across the rift zone, the earthquakes commonly initiate at the middle-crust and extend down into the lower crust, except the northwestern tip of the Rukwa Rift (Katavi sub-basin; Figs. 2a, 2d) where the earthquakes primarily localize within the upper crust (Lavayssière et al., 2019). More interestingly, the axis of the Rukwa Rift has sparse seismicity. Seismicity clusters at the Rukwa Rift tip extend beyond the margins of the basin sediments, continuing outboard into the regions of the exposed pre-rift basement (Figs. 2a and 2d). In the Tanganyika Rift, earthquakes mostly cluster within the rift axis and extend along most of

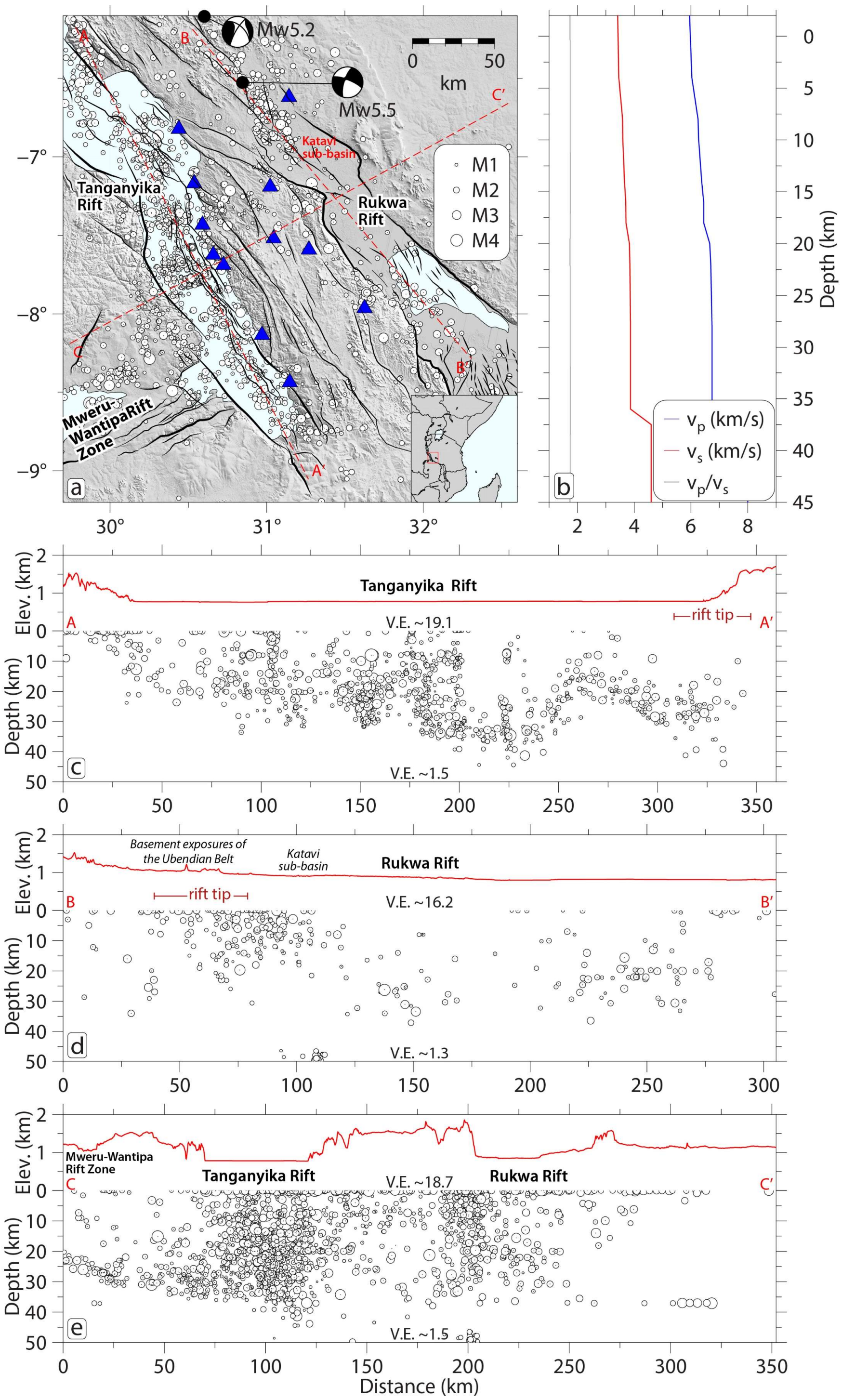

Figure 2. (**a**) Map of the southern Tanganyika and Rukwa rift zone showing the local seismicity (black circles) scaled by magnitude. The black dots represent events used in the inversion. Previously deployed broadband seismometers are the blue triangles. Black lines are faults; the thicker black lines highlight border faults. Red dashed lines are locations of seismicity profiles in c-e. Inset map shows the relative location in East Africa. (**b**) Starting model used in the seismic tomographic inversion. (**c** - **e**) Elevation and depth profiles showing projected seismicity along and across the rifts. Profiles A-A' and B-B' only show earthquakes within a 25 km.

the rift length (Figs. 2a and 2c). Heat flow measurements in the rift zone show thermal anomalies in the central Tanganyika Rift, the south-central region of the Rukwa Rift, and within the basement region ahead of the northwestern tip of the Rukwa Rift (Fig. 1a; Jones, 2020). The thermal anomaly north of the Rukwa Rift tip occurs near NW-trending fault splays and Mw>5 earthquake epicenters within the basement region. Furthermore, hydrothermal vent and hot spring locations coincide with the border fault zones of the Tanganyika Rift and the south-central part of the Rukwa Rift (Fig. 1a; Tiercelin et al., 1993; Lavayssière et al., 2019; Jones, 2020).

1.1.4 Active Deformation in Rift Overlap Zones

At a regional scale, the Rukwa and Tanganyika rift basins are separated by an elevated region of pre-rift basement with widespread exposures of Precambrian metamorphic rocks (Figs. 1a-b; Kolawole et al., 2021a). This region of rift overlap, described as an overlapping parallel-to-oblique 'rift interaction zone' (Kolawole et al., 2021), is characterized by historical seismicity and active faults that deform the modern surface (Delvaux et al., 2001; Lavayssière et al., 2019; Kolawole et al., 2021a). The faults are comprised of the WNW-trending Karema and Nkamba faults which splay westwards from the Rukwa Rift tip (Fig. 1a; Fernandez-Alonso et al., 2001; Kolawole et al., 2021a); and NW-trending faults that extend northwards towards the margin of the northern Tanganyika Rift (Kolawole et al., 2021a). The longitudinal surface relief morphology of the southern Tanganyika Rift shows a significantly steeper gradient than that of the Rukwa Rift tip ('rift tip' in Fig. 2c versus 2d). The asymmetricity of the relief profiles across the rift interaction zone, bidirectional axial stream flow from the zone into the rift basins, and the variation of drainage plan-form morphologies across the zone are interpreted to be controlled by a progressive northwestward encroachment of the subsidence axis of the Rukwa Rift (Kolawole et al., 2021a). Overall, the current stage of evolution of the rift interaction zone is inferred to be partially breached (Kolawole et al., 2021a).

The Mweru-Wantipa Rift extends eastward and appears to be hard-linked with the border fault of the western flank of the southern tip of the Tanganyika Rift. The region between the two rifts defines an overlapping orthogonal rift interaction zone (Kolawole et al., 2021a). The continuation of Lake Tanganyika into the Mweru-Wantipa Basin and the apparent coalescence of the rift floors of the two basins suggest a breached rift interaction zone between them (Kolawole et al., 2021a).

2 Data and Methods

2.1 Travel Time Dataset

We focus on data recorded by the TANGA14 array, comprising 13 broadband seismographs deployed along the Ufipa Plateau for 15 months from June 2014 through September 2015 (Hodgson et al., 2017). Travel time measurements were retrieved using the local seismicity catalog of Lavayssière et al. (2019) with 2213 events (Fig. 2a). First arrival times for both P and S waves were manually picked on filtered seismograms resulting in 3187 P times from 1277 earthquakes (resp. 3121 S times from 1261 earthquakes).

2.2 Body Wave Tomography

Using a one-dimensional (1-D) velocity model of the region as a starting model (Lavayssière et al., 2019), we iteratively introduce perturbations using the travel time picks. Predicted arrival times are computed by solving the eikonal equation (Vidale, 1990), and the corresponding model changes to the travel time residuals are found using the backprojection algorithm of Hole (1992). Due to the sparse station distribution, the model space is parameterized using a grid spacing of 5 km. Inversion regularization is achieved through varying smoothing sizes, which are changed every five iterations and decreases with increasing iterations. The final models are selected from the 26th iteration (Fig. 3) as subsequent models do not have substantially lower misfits but become contaminated from noise overfitting (Fig. S1). To assess the model uncertainty, we employ a combination of ray coverage maps and checkerboard reconstruction tests to determine areas of the model reliable enough for interpretation (Figs. 3 and S2 – S15).

3 Results

We present our preferred velocity models as perturbations (Fig. 3) relative to the starting physical model parameters used in the inversion (Fig. 2b) because the spatial resolution may cause the absolute values to be less reliable for interpretation (e.g., Figs. S4 – S15). The 5 km model grid spacing makes our selection of the 3 km depth maps (Figs. 3a, 3e, and 3i) representative of the average uppermost crustal structure of the model in the region, as can be verified in the cross-sectional profiles of Figure 3. The overall distribution of upper crustal velocities generally reflect the near-surface geology, which serves as a primary constraint for assessing the quality of the models.

Our results show that slower P (Vp) and S (Vs) wave velocities are collocated with the sedimentary basins of the southern Tanganyika and Rukwa rifts. Relatively lower velocities continue along a narrow ESE-trending zone from the Tanganyika Rift to the northern end of the Rukwa Rift, following the Nkamba and Karema faults. The Ufipa Horst separating the Tanganyika and Rukwa rifts also show localized zones of Lower P wave velocities, collocated with areas of pervasive surface faulting (Fig. 3a). However, unlike the P wave velocity distribution, the Ufipa Horst is better defined in the S wave velocity model, demonstrated by the relatively higher values and structural continuity (Figs. 3e and h). Within the eastern section of the Mweru-Wantipa Rift and futher east towards the southern Tanganyika Rift, we observe moderate Vp anomalies collocated with moderate to low Vs anomalies (Figs. 3a – b, e - f). Overall, the rift flanks and zones of widespread exposure of the pre-rift basement exhibit relatively higher P and S wave velocities.

The Vp/Vs ratio map (Fig. 3i) and cross-sections (Figs. 3j – l) show zones of anomalously high values that are restricted to upper-crustal depths, the most prominent of which are: 1) an anomaly at the northwestern end of the Rukwa Rift, an area dominated by basement exposures and distributed faulting, 2) an anomaly in the southeastern interior of the Rukwa Rift, collocated with the southeastern extension of the Precambrian Chisi Shear Zone (Fig. 1b), and 3) a broad anomaly extending across the eastern end of the Mweru-Wantipa Rift through the transfer zone into the Tanganyika Rift. These highest Vp/Vs anomalies commonly continue down to 10 km, except for the Mweru-Wantipa anomaly, which continues laterally into the southernmost sub-basin of the Tanganyika Rift, where it is strongly restricted to the sedimentary cover and shallow crystalline crust (<5 km; Fig. 3j). Although there are elevated Vp/Vs ratio anomalies at >17 km depths beneath the basins (Figures 3j – l), our investigation focuses on the upper crust.

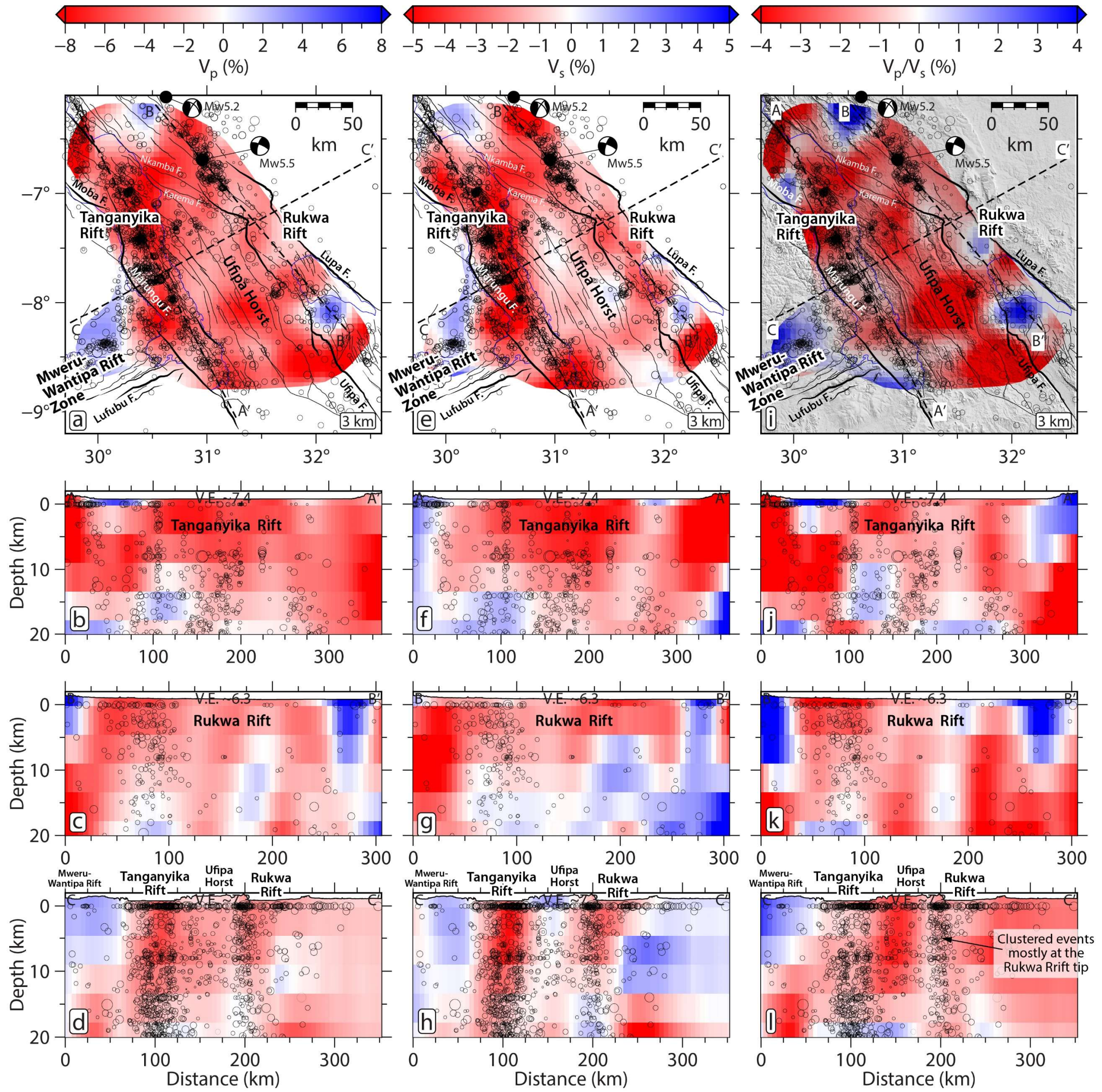

Figure 3. Maps and profiles through the tomographic models showing the perturbations relative to the starting models in Fig. 2b. (**a**) 3 km depth slice through the P wave velocity model. Unreliable areas of the model are not shown. Dashed black lines show the profile locations in b-d. (**b** – **d**) Profiles of the P wave velocity model. (**e** – **h**) Same as a-d but for the S wave velocity model. (**i** – **l**) Same as a-d but for the Vp/Vs ratios.

4 Discussion

Two of the three zones of the highest upper-crustal Vp/Vs ratios occur at rift tips where syn-rift sedimentary cover is thinnest and basement exposures dominate the surface geology (Rukwa and Mweru-Wantipa rift tips; Figs. 1b and 3i). These anomalies occur at or near known geothermal anomalies, including hot springs, hydrothermal vents, or high heat flow measurement sites (Fig. 1a). The anomalies are also collocated with earthquake clusters and distributed normal faults. The seismicity cluster at the tip is anomalous as it indicates the focus of active brittle deformation of the crystalline crust in a region lacking well-developed rift basins. At the Rukwa Rift tip and further to the northwest, the faulting pattern is generally characterized by splays of distributed faults that extend outboard from the Rukwa Rift border faults (Fig. 1a). At the Mweru-Wantipa Rift tip, the rift faults mainly cluster near the southern margin. Thus, we interpret the occurrence of the high upper-crustal Vp/Vs anomalies at the modern rift tips to represent a localization of mechanically weakened crystalline crust associated with brittle deformation and, potentially, compounded by the thermo-mechanical weakening effect of hydrothermal upwelling through fault-fracture networks. Studies have shown that anomalously high upper-crustal Vp/Vs anomalies in crystalline basement terranes are typical of localized zones of high intensity of fluid-saturated fracture networks, and zones of hydrothermally altered crustal rocks (Hauksson & Unruh, 2007). Geothermal anomalies activate voluminous hydrothermal upwelling, which often utilizes fracture networks as conduits (e.g., Pirajno, 2008), thus decreasing the bulk density and, consequently, the seismic velocity of the crust.

Localizing mechanically weakened crust at active rift tips reflects a critical process that drives the growth of continental rift systems. The northwestern tip of the Rukwa Rift is characterized by geomorphic features and tectonic deformation patterns that suggest an ongoing northwestward propagation towards the central and northern Tanganyika Rift (Kolawole et al., 2021a). However, an outstanding problem is the mechanism for strain localization ahead of the rift tip. Earthquake clustering at active rift tips (Fig. 2a) indicates focused strain and stress concentrations analogous to propagating microfractures (e.g., Martel, 1990; Kranz, 1979). At the rift scale, the intervening basement region between the Tanganyika and Rukwa rifts has been shown to represent a rift interaction zone (e.g., Nelson et al., 1991; Kolawole et al., 2021a). Similarly, the transfer zone between the Mweru-Wantipa and Tanganyika rifts, primarily composed of minor sedimentary cover (Fig. 1b) represents a rift interaction zone (Kolawole et al., 2021a). We argue that the rift interaction zones in the Rukwa-Tanganyika Rift Zone are localizing tectonic strain that may facilitate rift linkage and progressive dismembering of the intervening crystalline basement.

The location with a high Vp/Vs ratio in the central interior of the Rukwa Rift also lacks significant faulting relative to the nearby intra-rift areas (Fig. 3i). However, this anomaly is located along the southeastern continuation of the Precambrian Chisi Shear Zone in the crust beneath the Rukwa Rift sediments ('CSZ' in Fig. 1b; Lemna et al., 2019; Heilman et al., 2019; Kolawole et al., 2021b). This anomaly is near a region representing a paleo-rift tip in the earliest development phase of the Rukwa Rift during the Mesozoic (Kolawole et al., 2021b). Thus, since the high Vp/Vs anomaly is rooted in the upper crystalline crust (Fig. 3k), we interpret that it likely represents either an inherited geochemically altered and mechanically weak zone along the exhumed ductile shear zone, or a localized zone of fracturing that is inherited from the Mesozoic rift phases.

Published analog, numerical, and conceptual models for rift linkage demonstrate that rift basins can propagate laterally and interact when in proximity, leading to linkage and coalescence of the rifts (e.g., Allken et al., 2012; Corti, 2012; Molnar et al., 2019; Nelson et al., 1992; Zwaan et al., 2016; Zwaan & Schreurs, 2020; Neuharth et al., 2021; Kolawole et al., 2021a). Modelling and observational studies of natural rifts have also shown that inherited crustal mechanical barriers, nonoptimal rift interaction zone geometry, or unfavorable tectonic stress distribution can stall lateral rift propagation (e.g., van Wijk and Blackman, 2005; Kolawole et al., 2022, 2023; Shaban et al., 2023). In general, numerical models show that the stalling of a laterally propagating rift tip

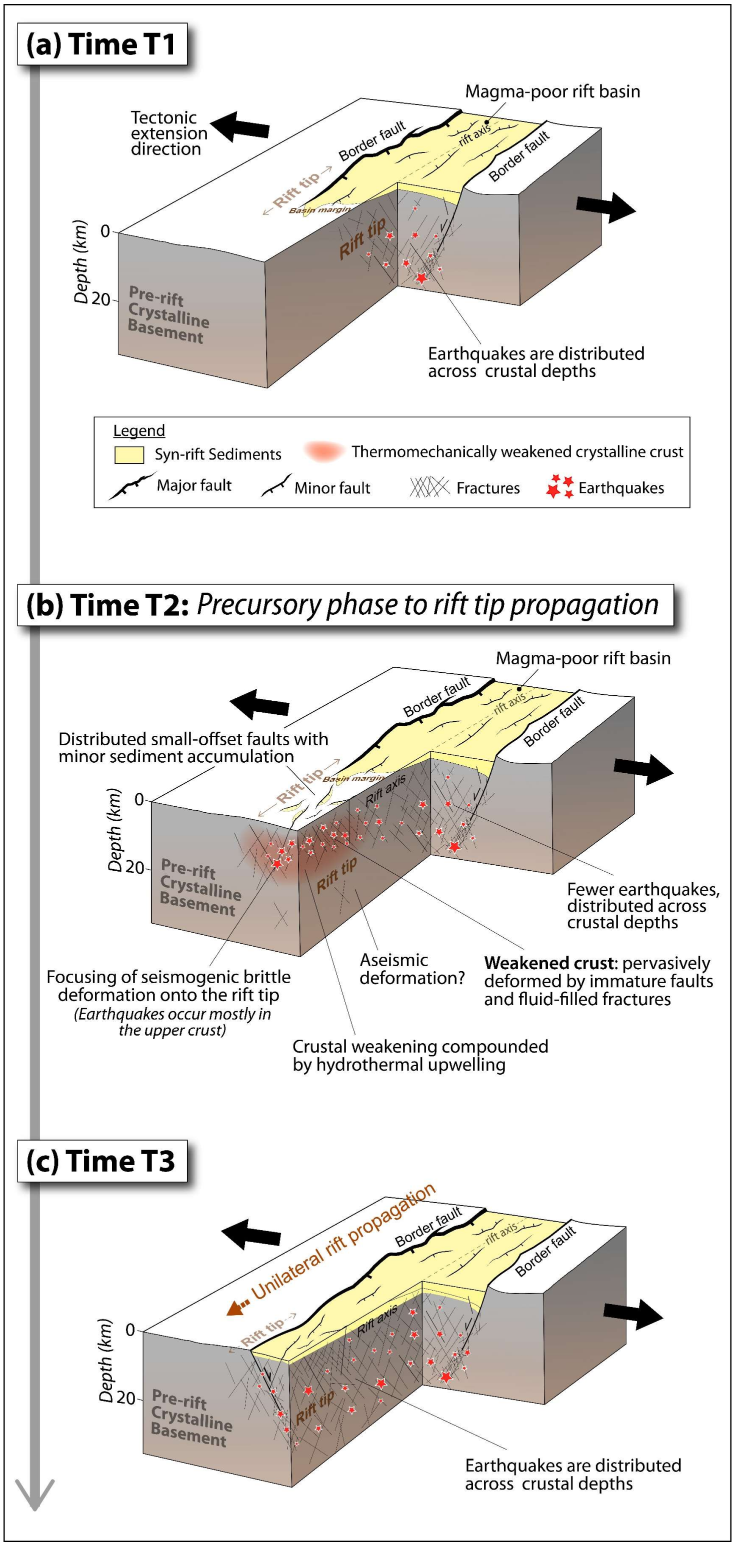

Figure 4. (**a – c**) Cartoons showing our proposed model of lateral propagation of an active continental rift basin and the patterns of crustal deformation at the rift tip as suggested by the results of this study. We show that a localized region of mechanically weakened crust develops ahead of the rift basin, facilitating the localization of strain onto regions of previously unrifted crust ahead of the basin.

creates a local zone of stress concentration or the development of a wide v-shaped zone of distributed deformation (van Wijk and Blackman, 2005; Le Pourhiet et al., 2018). To the best of our knowledge, the current geophysical study presents, for the first time, evidence from a natural rift, revealing localized weakening of a laterally propagating continental rift tip. Thus, we propose a new conceptual model for lateral rift propagation whereby before the inception of propagation, brittle deformation is generally distributed across the crust along the rift axis (Time T1, Fig. 4a). The inception of rift propagation is marked by an initial phase of stress concentration at the rift tip associated with seismogenic upper-crustal brittle damage (and aseismic deformation at depth?) with hydrothermal upwelling that eventually leads to the localized mechanical 'softening' of the crust (Time T2, Fig. 4b). Finally, the weakened crust gives way to the development of a well-established continuation of the border fault and rift basin ahead of the paleo-rift tip, and therefore, creats a new rift tip ahead of the previously weakened crust (Time T3, Fig. 4c).

Conclusions

To understand how tectonic strain is accommodated along active magma-poor continental rift zones, we constructed three-dimensional (3-D) velocity models of the crystalline crust beneath the Rukwa-Tanganyika Rift Zone, East Africa. The result that the highest Vp/Vs ratio anomalies are at the current and paleo rift tips represents, for the first time, geophysical evidence demonstrating that an initial crustal softening of the rift tip may be required to initiate unilateral rift propagation. Furthermore, we determine that localized geothermal anomalies and brittle damage facilitate the softening. These new results provide compelling insight into how continental rift tips interact, link, and coalesce to form continuous rift axial floors — a necessary ingredient for initiating large-scale continental break-up axis.

Acknowledgments

This project was supported by funds from the Columbia Climate School awarded to Folarin Kolawole. Some figures are plotted using the generic mapping tools (Wessel et al., 2019).

Author contributions

F.K. and R.A. conceptualized the project. R.A. analyzed the seismic data, performed the travel time inversion, and generated the body wave tomography images. F.K. and R.A. interpreted the results. F.K. wrote the the manuscript. R.A. revised the manuscript.

Competing interests

The authors declare no competing interests.

Open Research

The TANGA14 array data is available on IRIS DMC. We will make the computer programs and files needed to reproduce the results and figures publically available on Zenodo upon publication.

References

Allam, A. A., Ben-Zion, Y., Kurzon, I., & Vernon, F., 2014. Seismic velocity structure in the Hot Springs and Trifurcation areas of the San Jancinto fault zone, California, from double-difference tomography. Geophysical Journal International, 198, 978-999.

Ajala, R. & Persaud, P. (2021). Effect of Merging Multisclae Models on Seismic Wavefield Predictions Near the Southern San Andreas Fault. Journal of Geophysical Research: Solid Earth, 126, 1-23.

Allken, V., Huismans, R.S. and Thieulot, C., 2012. Factors controlling the mode of rift interaction in brittle-ductile coupled systems: A 3D numerical study. Geochemistry, Geophysics, Geosystems, 13(5).

Brune, S., Kolawole, F., Olive, J.A., Stamps, D.S., Buck, W.R., Buiter, S.J., Furman, T. and Shillington, D.J., 2023. Geodynamics of continental rift initiation and evolution. Nature Reviews Earth & Environment, 4(4), pp.235-253.

Cormier, V. F. & Spudich. (1984). Amplification of ground motion and waveform complexity in fault zones: examples from the San Andreas and Calaveras Faults. Geophys. J. R. astr. Soc., 79, 135–152.

Craig, T. J., Jackson, J. A., Priestley, K., & McKenzie, D. (2011). Earthquake distribution patterns in Africa: Their relationship to variations in lithospheric and geological structure, and their rheological implications. Geophysical Journal International, 185(1), 403–434. https://doi.org/10.1111/j.1365-246X.2011.04950.x

Delvaux, D., 1989. The Karoo to recent rifting in the western branch of the East-African Rift System: a bibliographical synthesis. In: Mus. Roy. Afr. Centr., Tervuren (Belg.), Dept. Geol. Min., Rapp. Ann, 1990, 1991, pp. 63–83.

Delvaux, D., & Barth, A. (2010). African stress pattern from formal inversion of focal mechanism data. Tectonophysics, 482(1–4), 105–128. https://doi.org/10.1016/j.tecto.2009.05.009.

Delvaux, D., Kervyn, F., Macheyeki, A. S., and Temu, E. B. (2012). Geodynamic Significance of the TRM Segment in the East African Rift (W-Tanzania): Active Tectonics and Paleostress in the Ufipa Plateau and Rukwa basin. J. Struct. Geology. 37, 161–180.

Ekstrom, D., Nettles, M., & Dziewonski, A. M. (2012). The global CMT project 2004-2010: Centroid-moment tensors for 13,017 earthquakes. Physics of the Earth and Planetary Interiors. 200-201, 1–9.

Fang, H., Yao, H., Zhang, H., Thurber, C., Ben-Zion, Y. and van der Hilst, R.D., 2019. V p/V s tomography in the southern California plate boundary region using body and surface wave traveltime data. Geophysical Journal International, 216(1), pp.609-620.

Foster, A. N., & Jackson, J. A. (1998). Source parameters of large African earthquakes: Implications for crustal rheology and regional kinematics. Geophysical Journal International, 134(2), 422–448. https://doi.org/10.1046/j.1365-246x.1998.00568.x

Gaherty, J.B., Zheng, W., Shillington, D.J., Pritchard, M.E., Henderson, S.T., Chindandali, P.R.N., Mdala, H., Shuler, A., Lindsey, N., Oliva, S.J. and Nooner, S., 2019. Faulting processes during early-stage rifting: Seismic and geodetic analysis of the 2009–2010 Northern Malawi earthquake sequence. Geophysical Journal International, 217(3), pp.1767-1782.

Ganbat, A., Tsujimori, T., Boniface, N., Pastor-Galán, D., Aoki, S. and Aoki, K., 2021. Crustal evolution of the Paleoproterozoic Ubendian Belt (SW Tanzania) western margin: a Central African Shield amalgamation tale. Gondwana Research, 91, pp.286-306.

Hauksson, E. & Unruh, J. (2007). Regional tectonics of the Coso geothermal area along the intracontinental plate boundary in central eastern California: three-dimensional Vp and Vp/Vs models, spatio-temporal seismicity patterns, and seismogenic deformation, Journal of Geophysical Research, 112(B6), 1-24.

Hanson, R.E., 2003. Proterozoic geochronology and tectonic evolution of southern Africa. Geological Society, London, Special Publications, 206(1), pp.427-463.

Heilman, E., Kolawole, F., Atekwana, E. A., and Mayle, M. (2019). Controls of Basement Fabric on the Linkage of Rift Segments. Tectonics 38 (4), 1337–1366. doi:10.1029/2018tc005362.

Hodgson, I., Illsley-Kemp, F., Gallacher, R., Keir, D., Ebinger, C. J., & Mtelela, K. (2017). Crustal Structure at a Young Continental Rift: A Receiver Function Study From the Tanganyika Rift. *Tectonics, 36*, 1-17.

Hole, J. A. (1992). Nonlinear high-resolution three-dimensional seismic travel time tomography. *Journal of Geophysical Research: Solid Earth, 97*(B5), 6553-6562. http://dx.doi.org/10.1029/92JB00235

Jones, D. J. R. (2020). A summary of the East Africa Rift Temperature and Heat flow Model (EARTH). British Geological Survey Open Report, OR/20/006. 24pp.

Kolawole, F., Firkins, M.C., Al Wahaibi, T.S., Atekwana, E.A. and Soreghan, M.J., 2021a. Rift interaction zones and the stages of rift linkage in active segmented continental rift systems. Basin Research, 33(6), pp.2984-3020.

Kolawole, F., Phillips, T.B., Atekwana, E.A. and Jackson, C.A.L., 2021b. Structural inheritance controls strain distribution during early continental rifting, rukwa rift. Frontiers in Earth Science, 9, p.707869.

Kolawole, F., Vick, T., Atekwana, E.A., Laó-Dávila, D.A., Costa, A.G., and Carpenter, B.M. (2022). Strain Localization and Migration During the Pulsed Lateral Propagation of the Shire Rift Zone, East Africa. Tectonophysics, 839, 229499. Doi: 10.1016/j.tecto.2022.229499.
Kolawole, F., Xue, L. and Dulanya, Z., 2023. Rapid Versus Delayed Linkage and Coalescence of Propagating Rift Tips. Authorea Preprints, 10.22541/essoar.168167202.29986035/v1.
Kranz, R. L. (1979). Crack-crack and crack-pore interactions in stressed granite. International Journal of Rock Mechanics and Mining Sciences & Geomechanics Abstracts, 16(1), 37–47.
Lavayssière, A., Drooff, C., Ebinger, C. J., Gallacher, R., Illsley-Kemp, F., Oliva, S. J., & Keir, D. (2019). Depth Extent and Kinematics of Faulting in the Southern Tanganyika Rift, Africa. *Tectonics, 38*, 842-862.
Lemna, O. S., Stephenson, R., and Cornwell, D. G. (2019). The Role of Pre-existing Precambrian Structures in the Development of Rukwa Rift Basin, Southwest Tanzania. J. Afr. Earth Sci. 150, 607–625. doi:10.1016/j.jafrearsci.2018.09.015.
Le Pourhiet, L., Chamot-Rooke, N., Delescluse, M., May, D.A., Watremez, L. and Pubellier, M., 2018. Continental break-up of the South China Sea stalled by far-field compression. Nature Geoscience, 11(8), pp.605-609.
Martel, S.J., 1990. Formation of compound strike-slip fault zones, Mount Abbot quadrangle, California. Journal of Structural Geology, 12(7), pp.869-882.
Molnar, N.E., Cruden, A.R. and Betts, P.G., 2019. Interactions between propagating rifts and linear weaknesses in the lower crust. Geosphere, 15(5), pp.1617-1640.
Morley, C. K., Cunningham, S. M., Harper, R. M., and Wescott, W. A. (1992). Geology and Geophysics of the Rukwa Rift, East Africa. Tectonics 11 (1), 69–81. doi:10.1029/91tc02102.
Morley, C. K., Wescott, W. A., Harper, R. M., and Cunningham, S. M. (1999). Geology and Geophysics of the Rukwa Rift. Geoscience of Rift Systems-Evolution of East Africa. AAPG Stud. Geology. 44, 91–110.
Muirhead, J. D., Wright, L. J., & Scholz, C. A. (2019). Rift evolution in regions of low magma input in East Africa. Earth and Planetary Science Letters, 506, 332–346.
Mulaya, E., Gluyas, J., McCaffrey, K., Phillips, T. & Ballentine, C. (2022). Structural geometry and evolution of the Rukwa Rift Basin, Tanzania: Implications for helium potential. Basin Research 34, 938-960.
Nelson, R.A., Patton, T.L. and Morley, C.K., 1992. Rift-segment interaction and its relation to hydrocarbon exploration in continental rift systems. AAPG bulletin, 76(8), pp.1153-1169.
Neuharth, D., Brune, S., Glerum, A., Heine, C. and Welford, J.K., 2021. Formation of continental microplates through rift linkage: Numerical modeling and its application to the Flemish Cap and Sao Paulo Plateau. Geochemistry, Geophysics, Geosystems, 22(4), p.e2020GC009615.
Pérez-Gussinyé, M., Collier, J.S., Armitage, J.J., Hopper, J.R., Sun, Z. and Ranero, C.R., 2023. Towards a process-based understanding of rifted continental margins. Nature Reviews Earth & Environment, 4(3), pp.166-184.
Pirajno, F., 2008. Hydrothermal processes and mineral systems. Springer Science & Business Media.
Roberts, E. M., Stevens, N. J., O'Connor, P. M., Dirks, P. H. G. M., Gottfried, M. D., Clyde, W. C., Armstrong, R. A., Kemp, A. I. S., & Hemming, S. (2012). Initiation of the western branch of the East African Rift coeval with the eastern branch. Nature Geoscience, 5(4), 289–294. https://doi.org/10.1038/ngeo1432.
Shaban, S., Scholz, C.A., Kolawole, F. (2023). The Deep Basin and Underlying Basement Structure of the Tanganyika Rift. Tectonics, 42, e2022TC007726.
Stamps, D. S., Calais, E., Saria, E., Hartnady, C., Nocquet, J. M., Ebinger, C. J., & Fernandes, R. M. (2008). A kinematic model for the East African Rift. Geophysical Research Letters, 35(5).
Stevens, V.L., Sloan, R.A., Chindandali, P.R., Wedmore, L.N., Salomon, G.W., Muir, R.A., 2021. The entire crust can be seismogenic: evidence from Southern Malawi. Tectonics 40 (6). https://doi.org/10.1029/2020TC006654 e2020TC006654.
Tiercelin, J.J., Pflumio, C., Castrec, M., Boulégue, J., Gente, P., Rolet, J., Coussement, C., Stetter, K.O., Huber, R., Buku, S. and Mifundu, W., 1993. Hydrothermal vents in Lake Tanganyika, East African, Rift system. Geology, 21(6), pp.499-502.
Van Wijk, J.K., Blackman, D.K., 2005. Dynamics of continental rift propagation: the endmember modes. Earth Planet. Sci. Lett. 229 (3–4), 247–258.
Veatch, A. C. (1935). Evolution of the Congo Basin. GSA Memoir 3.
Versfelt, J., & Rosendahl, B. (1989). Relationship between pre-rift structure and rift architecture in Lakes Tanganyika and Malawi, East Africa. Nature, 337, 354–357.
Vidale, J. E. (1990). Finite-difference calculation of traveltimes in three dimensions. *GEOPHYSICS, 55*(5), 521-526.
Wessel, P., Luis, J. F., Uieda, L., Scharroo, R., Wobbe, F., Smith, W. H. F., & Tian, D. (2019). The generic mapping tools version 6. Geochemistry, Geophysics, Geosystems, 20, 1-20. https://doi.org/10.1029/2019gc008515

Yang, Z., & Chen, W. P. (2010). Earthquakes along the East African Rift System: A multiscale, system-wide perspective. Journal of Geophysical Research, 115, B12309. https://doi.org/10.1029/2009JB006779

Zheng, W., Oliva, S.J., Ebinger, C. and Pritchard, M.E., 2020. Aseismic deformation during the 2014 M w 5.2 Karonga earthquake, Malawi, from satellite interferometry and earthquake source mechanisms. Geophysical Research Letters, 47(22), p.e2020GL090930.

Zwaan, F., & Schreurs, G. (2020). Rift segment interaction in orthogonal and rotational extension experiments: Implications for the large-scale development of rift systems. Journal of Structural Geology, 140, 104119. https://doi.org/10.1016/j.jsg.2020.104119

Zwaan, F., Schreurs, G., Naliboff, J., & Buiter, S. J. (2016). Insights into the effects of oblique extension on continental rift interaction from 3D analogue and numerical models. Tectonophysics, 693, 239–260. https://doi.org/10.1016/j.tecto.2016.02.036